9

Structure of Polycrystalline Aggregates

9–1 INTRODUCTION

In the previous chapter we were concerned with the orientation and quality of single crystals. But the normal way in which metals and alloys are produced and used is in the form of polycrystalline aggregates, composed of a great many individual crystals usually of microscopic size. Because the properties of such aggregates are of great technological importance, they have been intensively studied in many ways. In such studies the two most useful techniques are microscopic examination and x-ray diffraction, and the wise investigator will use them both; one complements the other, and both together can provide a great deal of information about the structure of an aggregate.

The properties (mechanical, electrical, chemical, etc.) of a single-phase aggregate are determined by two factors:

1) the properties of a single crystal of the material, and

2) the way in which the single crystals are put together to form the composite mass.

In this chapter we will be concerned with the second factor, namely, the *structure* of the aggregate, using this term in its broadest sense to mean the relative size, quality, and orientation of the grains making up the aggregate. Whether these grains are large or small, strained or unstrained, oriented at random or in some particular way, frequently has very important effects on the properties of the material.

If the aggregate contains more than one phase, its properties naturally depend on the properties of each phase considered separately and on the way these phases occur in the aggregate. Such a material offers wide structural possibilities since, in general, the size, quality, and orientation of the grains of one phase may differ from those of the other phase or phases.

CRYSTAL SIZE

9–2 GRAIN SIZE

The size of the grains in a polycrystalline metal or alloy has pronounced effects on many of its properties, the best known being the increase in strength and hardness which accompanies a decrease in grain size. This dependence of properties on

grain size makes the measurement of grain size a matter of some importance in the control of most metal forming operations.

The grain sizes encountered in commercial metals and alloys range from about 1000 to 1 μm. These limits are, of course, arbitrary and represent rather extreme values; typical values fall into a much narrower range, namely, about 100 to 10 μm. The most accurate method of measuring grain size in this range is by microscopic examination; the usual procedure is to determine the average number of grains per unit area of the polished section and report this in terms of an "index number" established by the American Society for Testing and Materials. The equation

$$n = 2^{N-1}$$

relates n, the number of grains per square inch when viewed at a magnification of 100×, and N, the ASTM "index number" or "grain-size number." Grain-size numbers of 4 and 8, for example, correspond to grain diameters of 90 and 22 μm, respectively.

Although x-ray diffraction is decidedly inferior to microscopic examination in the accurate measurement of grain size, one diffraction photograph can yield semi-quantitative information about grain size, *together with* information about crystal quality and orientation. A transmission or back-reflection pinhole photograph made with filtered radiation is best. If the back-reflection method is used, the surface of the specimen (which need not be polished) should be etched to remove any disturbed surface layer which might be present, because most of the diffracted radiation originates in a thin surface layer (see Secs. 9–4 and 9–5).

The nature of the changes produced in pinhole photographs by progressive reductions in specimen grain size is illustrated in Fig. 9–1. The governing effect here is the number of grains which take part in diffraction. This number is in turn related to the cross-sectional area of the incident beam, and its depth of penetration (in back reflection) or the specimen thickness (in transmission). When the grain size is quite coarse, as in Fig. 9–1(a), only a few crystals diffract and the photograph consists of a set of superimposed Laue patterns, one from each crystal, due to the white radiation present. A somewhat finer grain size increases the number of Laue spots, and those which lie on potential Debye rings generally are more intense than the remainder, because they are formed by the strong characteristic component of the incident radiation. Thus, the suggestion of Debye rings begins to appear, as in (b). When the grain size is further reduced, the Laue spots merge into a general background and only Debye rings are visible, as in (c). These rings are spotty, however, since not enough crystals are present in the irradiated volume of the specimen to reflect to all parts of the ring. A still finer grain size produces the smooth, continuous Debye rings shown in (d).

Several methods have been proposed for the estimation of grain size purely in terms of various geometrical factors. For example, an equation may be derived which relates the observed number of spots on a Debye ring to the grain size and other such variables as incident-beam diameter, multiplicity of the reflection, and specimen-film distance. However, many approximations are involved and the resulting equation is not very accurate. The best way to estimate grain size by

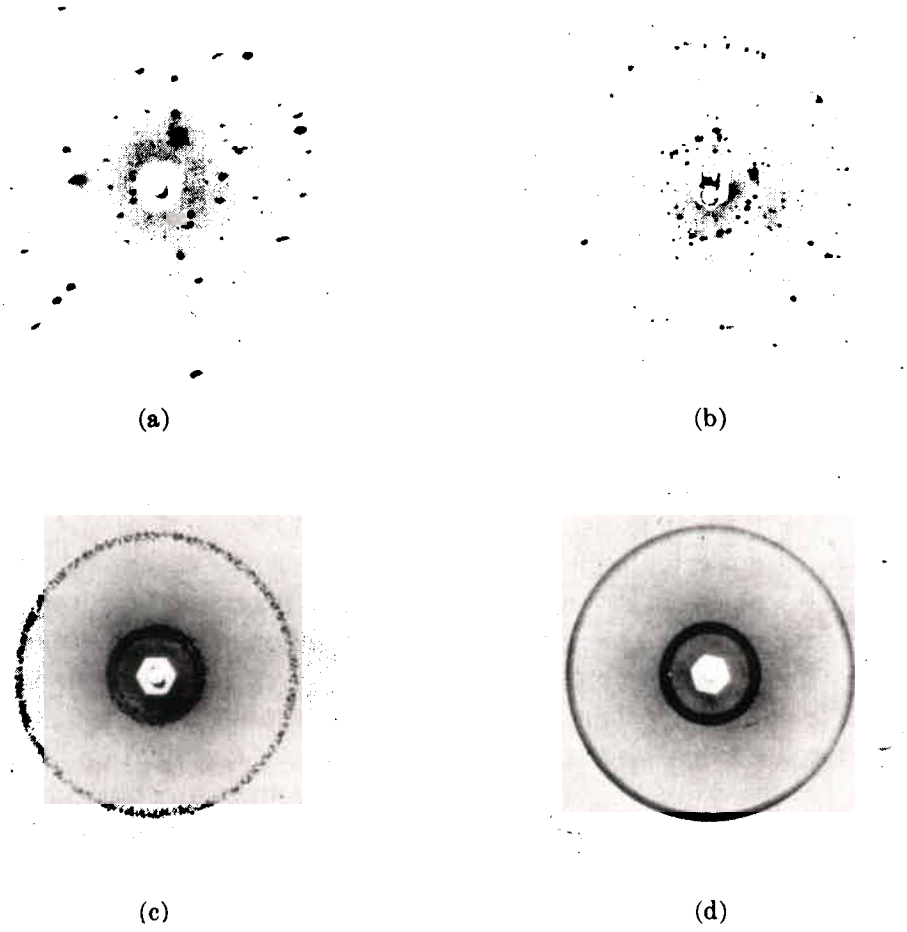

Fig. 9–1 Back-reflection pinhole patterns of recrystallized aluminum specimens; grain size decreases in the order (a), (b), (c), (d). Filtered copper radiation.

diffraction is to obtain a set of specimens having known ASTM grain-size numbers, and to prepare from these a standard set of photographs of the kind shown in Fig. 9–1. The grain-size number of an unknown specimen of the same material is then obtained simply by matching its diffraction pattern with one of the standard photographs, *provided both are made under identical conditions.*

When the grain size reaches a value somewhere in the range 10 to 1 μm, the exact value depending on experimental conditions, the Debye rings lose their spotty character and become continuous. Between this value and 0.1 μm (1000 Å), no change occurs in the diffraction pattern. At about 0.1 μm the first signs of line broadening, due to small crystal size, begin to be detectable. There is therefore a size range, from 10 (or 1) to 0.1 μm, where x-ray diffraction is quite insensitive to variations in grain size, at least for an incident beam of normal size. With microbeam techniques, x-ray lines remain spotty down to smaller grain sizes than are mentioned above, allowing spots from individual grains to be observed and counted [6.3].

9–3 PARTICLE SIZE

When the size of the individual crystals is less than about 0.1 μm (1000 Å), the term "particle size" is usually used. As we saw in Sec. 3–7, crystals in this size range cause broadening of the Debye rings, the extent of the broadening being given by Eq. (3–13):

$$B = \frac{0.9\lambda}{t \cos \theta}. \tag{3-13}$$

where B = broadening of diffraction line measured at half its maximum intensity (radians) and t = diameter of crystal particle. All diffraction lines have a measurable breadth, even when the crystal size exceeds 1000 Å, due to such causes as divergence of the incident beam and size of the sample (in Debye camerás) and width of the x-ray source (in diffractometers). The breadth B in Eq. (3–13) refers, however, to the *extra* breadth, or broadening, due to the particle-size effect alone. In other words, B is essentially zero when the particle size exceeds about 1000 Å.

The chief problem in determining particle size from line breadths is to determine B from the measured breadth B_M of the diffraction line. Of the many methods proposed, Warren's is the simplest. The unknown is mixed with a standard which has a particle size greater than 1000 Å, and which produces a diffraction line near that line from the unknown which is to be used in the determination. A diffraction pattern is then made of the mixture in either a Debye camera or, preferably, a diffractometer. This pattern will contain sharp lines from the standard and broad lines from the unknown, assumed to consist of very fine particles. Let B_S be the measured breadth, at half-maximum intensity, of the line from the standard. Then B is given, not simply by the difference between B_M and B_S, but by the equation

$$B^2 = B_M^2 - B_S^2. \tag{9-1}$$

(This equation results from the assumption that the diffraction line has the shape of an error curve [9.1].) Once B has been obtained from Eq. (9–1), it can be inserted into Eq. (3–13) to yield the particle size t. There are several other methods of finding B from B_M; compared with Warren's method, they are somewhat more accurate and considerably more intricate. These other methods involve Fourier analysis of the diffraction lines from the unknown and from the standard, and considerable computation [G.30, G.39]. Even the approach involving Eq. (9–1) can be difficult if the line from the standard is a resolved $K\alpha$ doublet; it is then simpler to use a $K\beta$ line. The Fourier methods automatically take care of the existence of a doublet.

Some investigators prefer to determine the *integral breadth* of a diffraction line rather than the breadth at half-maximum intensity. The integral breadth is given by the integrated intensity divided by the maximum intensity, i.e., it is the width of a rectangle having the same area and height as the observed line. Equation (9–1) is valid for both half-maximum and integral breadths.

The experimental difficulties involved in measuring particle size from line broadening increase with the size of the particle measured. Roughly speaking,

relatively crude measurements suffice in the range 0–500 Å, but very good experimental technique is needed in the range 500–1000 Å. The maximum size measurable by line broadening was formerly placed at 1000 Å, chiefly as a result of the use of camera techniques. With the diffractometer, however, the upper limit has been pushed to almost 2000 Å. Very careful work is required and back-reflection lines are employed, since such lines exhibit the largest particle-size broadening, as shown by Eq. (3–13).

From the above discussion it might be inferred that line broadening is chiefly used to measure the particle size of loose powders rather than the size of the individual crystals in a solid aggregate. That is correct. Attempts have been made to apply Eq. (3–13) to the broadened diffraction lines from very fine-grained metal specimens and so determine the size of the individual grains. Such determinations are never very reliable, however, because the individual grains of such a material are often nonuniformly strained, and this condition, as we shall see in the next section, can also broaden the diffraction lines; an uncertainty therefore exists as to the exact cause of the observed broadening. On the other hand, the individual crystals which make up a loose powder of fine particle size can often be assumed to be strain-free, provided the material involved is a brittle (nonplastic) one, and all the observed broadening can confidently be ascribed to the particle-size effect. (But note that loose, unannealed *metal* powders, produced by filing, grinding, ball milling, etc., almost always contain nonuniform strain.) The chief applications of the line-broadening method have been in the measurement of the particle size of such materials as carbon blacks, catalysts, and industrial dusts.

Another x-ray method of measuring the size of small particles deserves some mention, although a complete description is beyond the scope of this book. This is the method of *small-angle scattering*. It is a form of diffuse scattering very near the undeviated transmitted beam, i.e., at angles 2θ ranging from 0° up to roughly 2 or 3°. From the observed variation of the scattered intensity vs. angle 2θ, the size, and to some extent the shape, of small particles can be determined, whether they are amorphous or crystalline [G.15, G.21, 9.2]. Small-angle scattering has also been used to study precipitation effects in metallic solid solutions.

CRYSTAL QUALITY

9–4 CRYSTAL QUALITY

Of the many kinds of crystal imperfection, the one we are mainly concerned with here is nonuniform strain because it is so characteristic of the *cold-worked state* of metals and alloys. When a polycrystalline piece of metal is plastically deformed, for example by rolling, slip occurs in each grain and the grain changes its shape, becoming flattened and elongated in the direction of rolling. The change in shape of any one grain is determined not only by the forces applied to the piece as a whole, but also by the fact that each grain retains contact on its boundary surfaces with all its neighbors. Because of this interaction between grains, a single grain in a polycrystalline mass is not free to deform in the same way as an isolated crystal

would, if subjected to the same deformation by rolling. As a result of this restraint by its neighbors, a plastically deformed grain in a solid aggregate usually has regions of its lattice left in an elastically bent or twisted condition or, more rarely, in a state of uniform tension or compression. The metal is then said to contain *residual stress*. (Such stress is often called "internal stress" but the term is not very informative since all stresses, residual or externally imposed, are internal. The term "residual stress" emphasizes the fact that the stress remains after all external forces are removed.) Stresses of this kind are also called *microstresses* since they vary from one grain to another, or from one part of a grain to another part, on a microscopic scale. On the other hand, the stress may be quite uniform over large distances; it is then referred to as *macrostress*.

The effect of strain, both uniform and nonuniform, on the direction of x-ray reflection is illustrated in Fig. 9-2. A portion of an unstrained grain appears in (a) on the left, and the set of transverse reflecting planes shown has everywhere its equilibrium spacing d_0. The diffraction line from these planes appears on the right. If the grain is then given a uniform tensile strain at right angles to the reflecting planes, their spacing becomes larger than d_0, and the corresponding diffraction line shifts to lower angles but does not otherwise change, as shown in (b). This line shift is the basis of the x-ray method for the measurement of macrostress, as will be described in Chap. 16. In (c) the grain is bent and the strain is nonuniform; on the top (tension) side the plane spacing exceeds d_0, on the bottom (compression) side it is less than d_0, and somewhere in between it equals d_0. We may imagine this grain to be composed of a number of small regions in each of which the plane spacing is substantially constant but different from the spacing in adjoining regions. These regions cause the various sharp diffraction lines indicated on the right of (c) by the dotted curves. The sum of these sharp lines, each slightly displaced from the other, is the broadened diffraction line shown by the full curve and, of course, the broadened line is the only one experimentally observable. We can find a relation between the broadening produced and the nonuniformity of the strain by differentiating the Bragg law. We obtain

$$b = \Delta 2\theta = -2\frac{\Delta d}{d}\tan\theta, \tag{9-2}$$

where b is the extra broadening, over and above the instrumental breadth of the line, due to a fractional variation in plane spacing $\Delta d/d$. This equation allows the variation in strain, $\Delta d/d$, to be calculated from the observed broadening. This value of $\Delta d/d$, however, includes both tensile and compressive strain and must be divided by two to obtain the maximum tensile strain alone, or maximum compressive strain alone, if these two are assumed equal. The maximum strain so found can then be multiplied by the elastic modulus E to give the maximum stress present.

When an annealed metal or alloy is cold worked, its diffraction lines become broader. This is a well-established, easily verified experimental fact, but its explanation was for many years a matter of controversy. Some investigators felt that the chief effect of cold work was to fragment the grains to a point where their

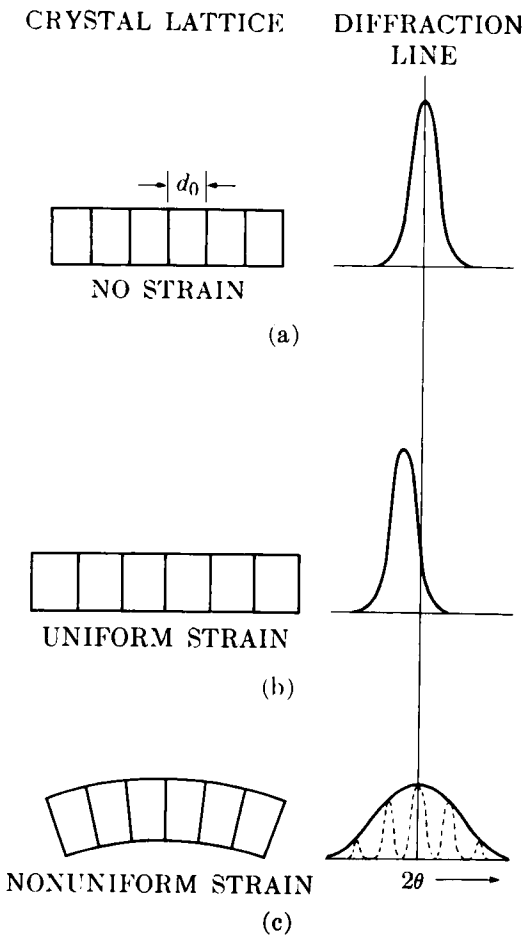

Fig. 9–2 Effect of lattice strain on Debye-line width and position.

small size alone was sufficient to account for all the observed broadening. Others concluded that the nonuniformity of strain produced by cold work was the major cause of broadening, with grain fragmentation possibly a minor contributing cause. This controversy revolved around the measurement of line widths and their interpretation in terms of either "particle-size broadening," according to Eq. (3–13), or "strain broadening," Eq. (9–2).

In 1949, however, Warren pointed out that there was important information about the state of a cold-worked metal in the *shape* of its diffraction lines, and that to base conclusions only on line *width* was to use only part of the experimental evidence. If the observed line profiles, corrected for instrumental broadening, are expressed as Fourier series, then an analysis of the Fourier coefficients discloses both particle size and strain, without the necessity for any prior assumption as to the existence of either [9.3, G.30, G.39]. Warren and Averbach [9.4] made the first measurements of this kind, on brass filings, and many similar studies followed [9.5]. Somewhat later, Paterson [9.6] showed that the Fourier coefficients of the line profile could also disclose the presence of stacking faults caused by cold work. (In FCC metals and alloys, for example, slip on {111} planes can here and there alter the normal stacking sequence $ABCABC\ldots$ of these planes to the faulted

sequence *ABCBCA* . . . .) Thus three causes of line broadening are now recognized: small particle size, nonuniform strain, and stacking faults.

These studies of line shape showed that it was impossible to generalize about the causes of line broadening in cold-worked metals and alloys. In some materials all three causes contribute, in others only one. But there appears to be no material for which all the observed broadening can be ascribed to fine particle size. In fact, it is difficult to imagine how cold work could fragment the grains to the degree necessary to cause particle-size broadening without at the same time introducing nonuniform strains, in view of the very complex forces that must act on any one grain of an aggregate no matter how simple the forces applied to the aggregate as a whole.

The broadening of a diffraction line by cold work cannot always be observed by simple inspection of a photograph unless some standard is available for comparison. However, the separation of the $K\alpha$ doublet furnishes a very good "internal standard." In the back-reflection region, an annealed metal produces a well-resolved doublet, one component due to $K\alpha_1$ radiation and the other to $K\alpha_2$. For a given set of experimental conditions, the separation of this doublet on the film is constant and independent of the amount of cold work. But as the amount of cold work is increased, the broadening increases, until finally the two components of the doublet overlap to such an extent that they appear as one unresolved line. An unresolved $K\alpha$ doublet can therefore be taken as evidence of cold work, if the same doublet is resolved when the metal is in the annealed condition.

We are now in a position to consider some of the diffraction effects associated with the processes of *recovery*, *recrystallization*, and *grain growth*. When a cold-worked metal or alloy is annealed at a low temperature, recovery takes place; at a somewhat higher temperature, recrystallization; and at a still higher temperature, grain growth. Or at a sufficiently high constant temperature, these processes may be regarded as occurring consecutively in time. During recovery, both macro and micro residual stress are reduced in magnitude, but the strength and hardness remain high; much of this stress relief appears to be due to polygonization, which can occur in the individual grains of an aggregate just as in a single crystal. During recrystallization, new grains form, residual stress is practically eliminated, and strength and hardness decrease rather abruptly.

Because the nonuniform strain due to residual microstress is the major cause of line broadening, we usually find that the broad diffraction lines characteristic of cold-worked metal partially sharpen during recovery. When recrystallization occurs, the lines attain their maximum sharpness. During grain growth, the lines become increasingly spotty as the grain size increases.

The hardness curve and diffraction patterns of Fig. 9-3 illustrate these changes for an alpha brass, a solid solution of zinc in copper, containing 30 percent zinc by weight. The hardness remains practically constant, for an annealing period of one hour, until a temperature of 200°C is exceeded, and then decreases rapidly with increasing temperature, as shown in (a). The diffraction pattern in (b) exhibits the broad diffuse Debye lines produced by the cold-rolled, unannealed alloy. These lines become somewhat narrower for specimens annealed at 100° and 200°C, and the $K\alpha$ doublet becomes partially resolved at 250°C. At 250°, therefore, the re-

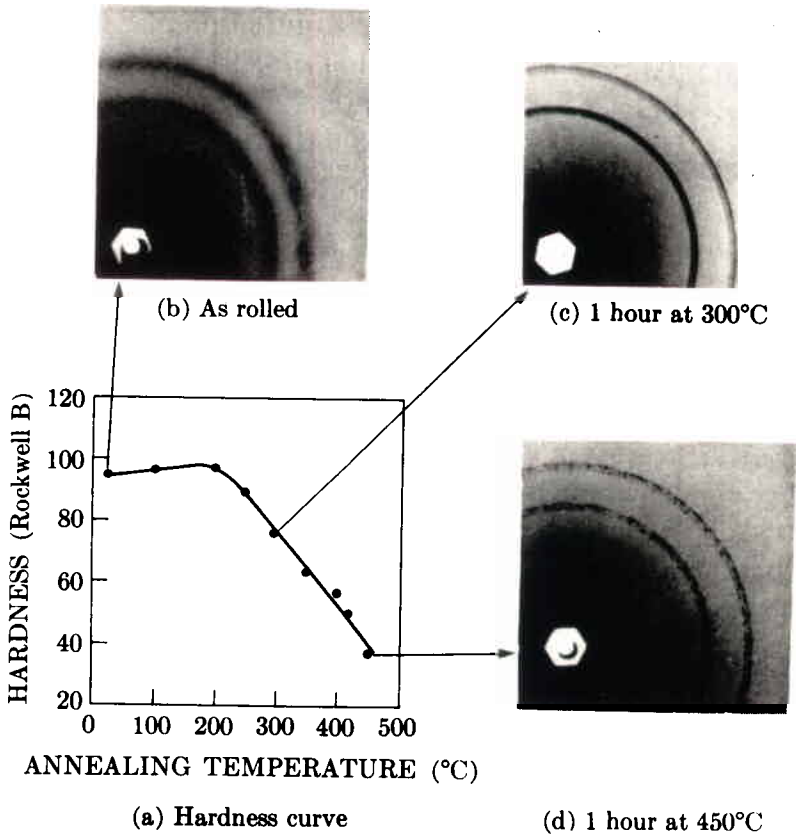

Fig. 9–3 Changes in hardness and diffraction lines of 70 Cu–30 Zn specimens, reduced in thickness by 90 percent by cold rolling, and annealed for 1 hour at the temperatures indicated in (a). (b), (c), and (d) are portions of back-reflection pinhole patterns of specimens annealed at the temperatures stated (filtered copper radiation).

covery process appears to be substantially complete in one hour and recrystallization is just beginning, as evidenced by the drop in Rockwell B hardness from 98 to 90. At 300°C the diffraction lines are quite sharp and the doublets completely resolved, as shown in (c). Annealing at temperatures above 300°C causes the lines to become increasingly spotty, indicating that the newly recrystallized grains are increasing in size. The pattern of a specimen annealed at 450°C, when the hardness had dropped to 37 Rockwell B, appears in (d).

Diffractometer measurements made on the same specimens disclose both more, and less, information. Some automatically recorded profiles of the 331 line, the outer ring of the patterns shown in Fig. 9–3, are reproduced in Fig. 9–4. It is much easier to follow changes in line shape by means of these curves than by inspection of pinhole photographs. Thus the slight sharpening of the line at 200°C is clearly evident in the diffractometer record, and so is the doublet resolution which occurs at 250°C. But note that the diffractometer cannot "see" the spotty diffraction lines caused by coarse grains. There is nothing in the diffractometer records made at 300° and 450°C which would immediately suggest that the specimen annealed at 450°C had the coarser grain size, but this fact is quite evident in the pinhole patterns shown in Figs. 9–3(c) and (d).

If an x-ray camera is not available, a piece of dental film can be placed just in

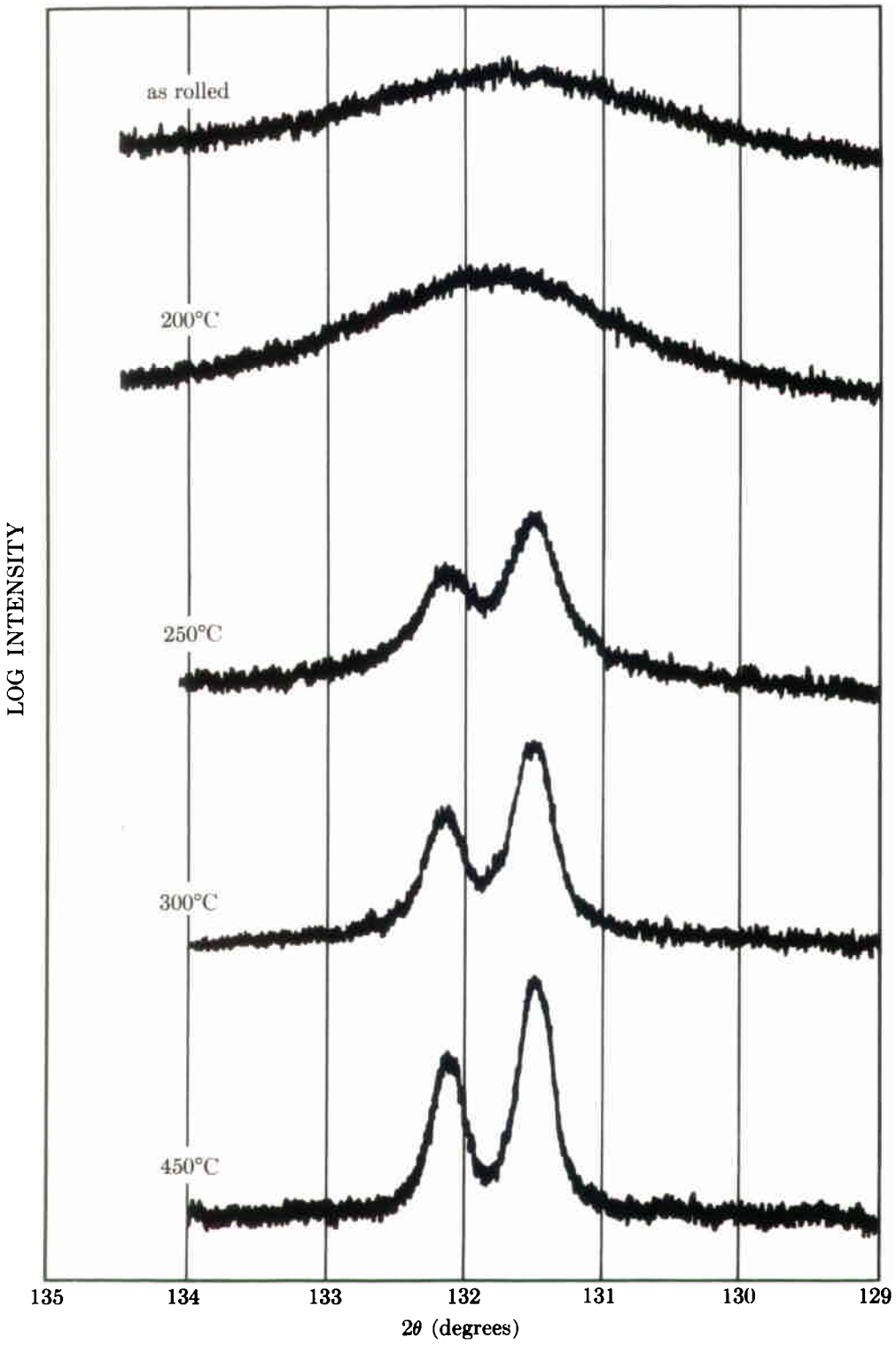

Fig. 9–4 Diffractometer traces of the 331 line of the cold-rolled and annealed 70–30 brass specimens referred to in Fig. 9–3. Filtered copper radiation. Logarithmic intensity scale. All curves displaced vertically by arbitrary amounts.

front of the counter slit of the diffractometer to disclose whether or not the diffraction lines are spotty. (Dental x-ray film, available from dental supply houses, comes in the form of a single piece of film, typically about 4 × 5 cm, enclosed in a thin envelope of light-tight plastic.) If a diffraction line is spotty on a photograph, the grain size of the specimen is too large for accurate intensity measurements with the diffractometer.

Figures 9–3 and 9–4 illustrate line sharpening by annealing. Conversely, when an annealed metal is progressively deformed, the x-ray lines progressively broaden and the hardness increases. In fact, the hardness of a particular metal or alloy can be rather accurately measured from the breadth of its diffraction lines. The relation between line breadth and hardness is not general, but must be determined experimentally for each particular material. (Very slight degrees of deformation can be detected by observation of the $K\alpha$ doublet. Rather than attempting to measure a slight increase in line width, one measures the ratio of the height of the "valley" between $K\alpha_1$ and $K\alpha_2$ to the height of $K\alpha_2$. This ratio increases rapidly as the lines broaden.)

When steel is hardened by quenching, the x-ray lines become very broad because of the microstrains due to the formation of martensite. Subsequent tempering causes progressive softening and line sharpening. Here again, a useful relation can be established experimentally between line width and hardness, applicable to a particular type of steel. (A rapid method of determining line width from the measurements used to determine residual stress is given in Sec. 16–4.)

Line-width observations are nearly always made in back reflection, whether by a photographic technique (Fig. 9–3) or by the diffractometer (Fig. 9–4). It is then necessary to remember that the observation applies only to a thin surface layer of the specimen. For example, Fig. 9–5(a) was obtained from a piece of copper and exhibits unresolved doublets in the high-angle region. The inexperienced observer might conclude that this material was highly cold worked. What the x-ray "sees" *is* cold worked, but it sees only to a limited depth. Actually, the bulk of this specimen is in the annealed condition, but the surface from which the x-ray pattern was made had had 50 μm removed by grinding on a belt sander after annealing. This treatment cold worked the surface to a considerable depth. By successive

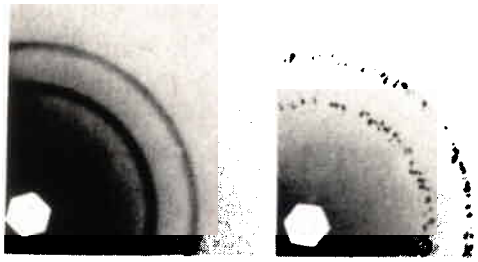

(a) (b)

Fig. 9–5 Back-reflection pinhole patterns of coarse-grained recrystallized copper. Unfiltered copper radiation: (a) from surface ground on a belt sander; (b) after removal of 0.003 in. (75 μm) from this surface by etching.

etching treatments and diffraction patterns made after each etch, the change in structure of the cold-worked layer could be followed as a function of depth below the ground surface. Not until a total of 75 μm had been removed did the diffraction pattern become characteristic of the bulk of the material; see Fig. 9–5(b), where the spotty lines indicate a coarse-grained, recrystallized structure.

9–5 DEPTH OF X-RAY PENETRATION

Observations of this kind suggest that it might be well to consider in some detail the general problem of x-ray penetration. Most metallurgical specimens strongly absorb x-rays, and the intensity of the incident beam is reduced almost to zero in a very short distance below the surface. The diffracted beams therefore originate chiefly in a thin surface layer whenever a reflection technique, as opposed to a transmission technique, is used, i.e., whenever a diffraction pattern is obtained in a back-reflection camera of any kind, a Seemann–Bohlin camera, or a diffractometer as normally used. We have just seen how a back-reflection pinhole photograph of a ground surface discloses the cold-worked condition of a thin surface layer and gives no information whatever about the bulk of the material below that layer.

These circumstances naturally pose the following question: what is the effective depth of x-ray penetration? Or, stated in a more useful manner, to what depth of the specimen does the information in such a diffraction pattern apply? This question has no precise answer because the intensity of the incident beam does not suddenly become zero at any one depth but rather decreases exponentially with distance below the surface. However, we can obtain an answer which, although not precise, is at least useful, in the following way. Equation (4–14) gives the integrated intensity diffracted by an infinitesimally thin layer located at a depth x below the surface as

$$dI_D = \frac{I_0 ab}{\sin \gamma} e^{-\mu x(1/\sin\gamma + 1/\sin\beta)}\, dx, \qquad (4\text{–}14)$$

where the various symbols are defined in Sec. 4–10. This expression, integrated over any chosen depth of material, gives the total integrated intensity diffracted by that layer, but only in terms of the unknown constants I_0, a, and b. However, these constants will cancel out if we express the intensity diffracted by the layer considered as a fraction of the total integrated intensity diffracted by a specimen of infinite thickness. (As we saw in Sec. 4–10, "infinite thickness" amounts to only a few thousandths of an inch for most metals.) Call this fraction G_x. Then

$$G_x = \frac{\int_{x=0}^{x=x} dI_D}{\int_{x=0}^{x=\infty} dI_D} = [1 - e^{-\mu x(1/\sin\gamma + 1/\sin\beta)}]. \qquad (9\text{–}3)$$

This expression permits us to calculate the fraction G_x of the total diffracted intensity which is contributed by a surface layer of depth x. If we arbitrarily decide that a contribution from this surface layer of 95 percent (or 99 or 99.9 percent) of the total is enough so that we can ignore the contribution from the material below that layer, then x is the effective depth of penetration. We then know that the

information recorded on the diffraction pattern (or, more precisely, 95 percent of the information) refers to the layer of depth x and not to the material below it.

In the case of the diffractometer, $\gamma = \beta = \theta$, and Eq. (9–3) reduces to

$$G_x = (1 - e^{-2\mu x/\sin\theta}), \tag{9–4}$$

which shows that the effective depth of penetration decreases as θ decreases and therefore varies from one diffraction line to another. In back-reflection cameras, $\gamma = 90°$, and

$$G_x = [1 - e^{-\mu x(1 + 1/\sin\beta)}], \tag{9–5}$$

where $\beta = 2\theta - 90°$.

For example, the conditions applicable to the outer diffraction ring of Fig. 9–5 are $\mu = 473\ \text{cm}^{-1}$ and $2\theta = 136.7°$. By using Eq. (9–5), we can construct the plot of G_x as function of x which is shown in Fig. 9–6. We note that 95 percent of the information on the diffraction pattern refers to a depth of only about 25 μm. It is therefore not surprising that the pattern of Fig. 9–5(a) discloses only the presence of cold-worked metal, since we found by repeated etching treatments that the depth of the cold-worked layer was about 75 μm. Of course, the information recorded on the pattern is heavily weighted in terms of material just below the surface; thus 95 percent of the recorded information applies to a depth of 25 μm, but 50 percent of *that* information originates in the first 5 μm. (Note that an effective penetration of 25 μm means that a surface layer only one grain thick is effectively contributing to the diffraction pattern if the specimen has an ASTM grain-

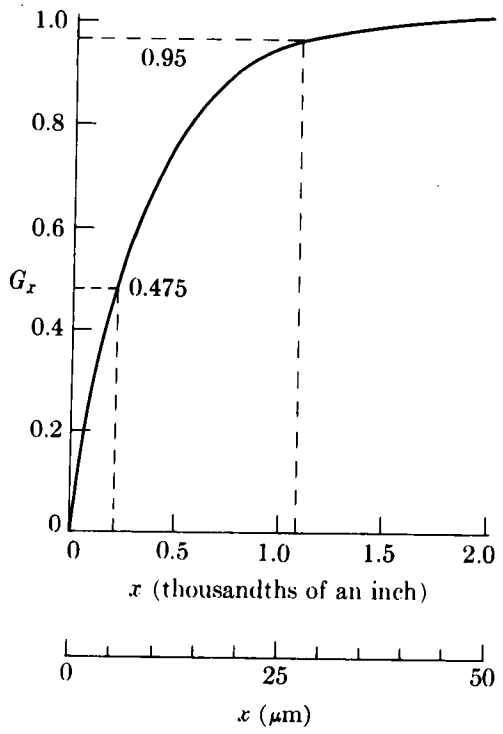

Fig. 9–6 The fraction G_x of the total diffracted intensity contributed by a surface layer of depth x, for $\mu = 473\ \text{cm}^{-1}$, $2\theta = 136.7°$, and normal incidence.

size number of 8. This layer contains some 300,000 reflecting lattice planes for the 331 diffraction line considered here.)

Equation (9–4) can be put into the following form, which is more suitable for calculation:

$$\frac{2\mu x}{\sin\theta} = \ln\left(\frac{1}{1 - G_x}\right) = K_x,$$

$$x = \frac{K_x \sin\theta}{2\mu}. \qquad \text{[Diffractometer]}$$

Similarly, we can rewrite Eq. (9–5) in the form

$$\mu x\left(1 + \frac{1}{\sin\beta}\right) = \ln\left(\frac{1}{1 - G_x}\right) = K_x,$$

$$x = \frac{K_x \sin\beta}{\mu(1 + \sin\beta)}. \qquad \text{[Back-reflection camera]}$$

Values of K_x corresponding to various assumed values of G_x are given in Table 9–1.

Table 9-1

G_x	0.50	0.75	0.90	0.95	0.99	0.999
K_x	0.69	1.39	2.30	3.00	4.61	6.91

Calculations of the effective depth of penetration can be valuable in many applications of x-ray diffraction. We may wish to make the effective depth of penetration as large as possible in some applications. Then γ and β in Eq. (9–3) must be as large as possible, indicating the use of high-angle lines, and μ as small as possible, indicating short-wavelength radiation. Other applications may demand very little penetration, as when we wish information, e.g., chemical composition or lattice parameter, from a very thin surface layer. Then we must make μ large, by using radiation which is highly absorbed, and γ and β small, by using a diffractometer at low values of 2θ.* By these means the depth of penetration can often be made surprisingly small. For instance, if a steel specimen is examined in a diffractometer with Cu $K\alpha$ radiation, 95 percent of the information afforded by the lowest angle line of ferrite (the 110 line at $2\theta = 45°$) applies to a depth of only 2 μm. There are limits, of course, to reducing the depth of x-ray penetration, and when information is required from very thin surface films, electron diffraction is a far more suitable tool (see Appendix 2).

* Some of these requirements may be contradictory. For example, in measuring the lattice parameter of a thin surface layer with a diffractometer, we must compromise between the low value of θ required for shallow penetration and the high value of θ required for precise parameter measurements.

Although the diffracted beam in any reflection method comes only from a very thin surface layer, it must not be supposed that the information on a diffraction pattern obtained by a transmission method is truly representative of the entire cross section of the specimen. Calculations such as those given above show that a greater proportion of the total diffracted energy originates in a layer of given thickness on the back side of the specimen (the side from which the transmitted beam leaves) than in a layer of equal thickness on the front side. If the specimen is highly absorbing, a transmission method can be almost as nonrepresentative of the entire specimen as a back-reflection method, in that most of the diffracted energy will originate in a thin surface layer. See Problem 9–5.

CRYSTAL ORIENTATION

9–6 GENERAL

Each grain in a polycrystalline aggregate normally has a crystallographic orientation different from that of its neighbors. Considered as a whole, the orientations of all the grains may be randomly distributed in relation to some selected frame of reference, or they may tend to cluster, to a greater or lesser degree, about some particular orientation or orientations. Any aggregate characterized by the latter condition is said to have a *preferred orientation*, or *texture*, which may be defined simply as a condition in which the distribution of crystal orientations is nonrandom.

Preferred orientation is a very common condition. Among metals and alloys it is most evident in wire and sheet, and the kinds of texture found in these products are dealt with below. The preferred orientation that is produced by the forming process itself (wire drawing or sheet rolling) is called a *deformation texture*. It is due to the tendency of the grains in a polycrystalline aggregate to rotate during plastic deformation; each grain undergoes slip and rotation in a complex way that is determined by the imposed forces and by the slip and rotation of adjoining grains; the result is a preferred, nonrandom orientation. When the cold-worked metal, possessed of a deformation texture, is recrystallized by annealing, the new grain structure usually has a preferred orientation too, often different from that of the cold-worked material. This is called a *recrystallization texture* or *annealing texture*. It is due to the influence which the texture of the cold-worked matrix has on the nucleation and/or growth of the new grains in that matrix.

Preferred orientation is not confined to metallurgical products. It also exists in rocks, ceramics, and in both natural and artificial polymeric fibers and sheets. In fact, preferred orientation is generally the rule, not the exception, and the preparation of an aggregate with completely random crystal orientations is a difficult matter.

The industrial importance of preferred orientation lies in the effect, often very marked, which it has on the overall, macroscopic properties of materials. Given the fact that all single crystals are anisotropic, i.e., have different properties in different directions, it follows that an aggregate having preferred orientation must also have directional properties to a greater or lesser degree. Such properties may